**Mariusz PAULUK**

AGH University of Science and Technology

doi:10.15199/48.2016.02.53

# Optimal and robust control of 3D crane

***Streszczenie.*** *W artykule zaprezentowano wyniki rozważań na temat możliwości optymalno-czasowego sterowania suwnicą 3D. Zaimplementowano ideę optymalnych trajektorii sąsiadujących w celu zapewnienia odporności sterowania optymalno-czasowego, obliczonego na podstawie nieliniowego modelu. Regulator LQ nadzoruje proces regulacji i dodatkowo eliminuje niepożądane własności trajektorii optymalnej. Zamieszczono krótkie omówienie wyników eksperymentalnych przeprowadzonych zarówno w otwartej jak i zamkniętej pętli sterowania.* ***Możliwości optymalno-czasowego sterowania suwnicą 3D***

***Abstract****. This paper concerns the time-optimal control of 3D crane, based on a tenth order nonlinear mathematical model. The idea of neighboring optimal trajectories is employed to ensure robustness of the time-optimal control calculated for the nonlinear model. An LQ controller supervises the control process and additionally eliminates unwanted properties of the optimal trajectory. The results of open-loop and closed-loop experiments are discussed.*

**Słowa kluczowe**: suwnica 3D, sterowanie w czasie rzeczywistym, sterowanie optymalno-czasowe, regulator LQ,
**Keywords**: 3D crane, real time control, time optimal control, LQ controller

## Introduction

A crane control task almost always relies on a trade-off between the time of transport and payload oscillations. Usually, faster transport causes greater swings of the payload which forces the operator to slow down the crane cart. An additional factor which makes the cranes working in open air slower are winds. It is thus natural that good solutions of the crane control problem are such that move the payload along a time-optimal trajectory with oscillations as small as possible, and the control algorithm is robust to disturbances.

In many papers 2D crane models are considered [1][6]. The presented controllers are usually based on linear models and it is assumed that the oscillations of the payload are so small that the trigonometric relations may be neglected [1][5]. This level of accuracy may be unsatisfying when the time-optimal solution is needed [7][9]. Frequently, the time-optimal controls are of bang-bang character [6][8]. The greater the admissible oscillations, the more effective the time-optimal controller and in consequence, the swings of the payload may be so large that the above assumption is no longer valid.

This paper concerns the time-optimal control of 3D crane, based on a tenth order nonlinear mathematical model. The idea of neighboring optimal trajectories is employed to ensure robustness of the time-optimal control calculated for the nonlinear model [9]-[12]. An LQ controller supervises the control process and additionally eliminates unwanted properties of the optimal trajectory. Its parameters (entries of a 3 x 10 matrix) are computed with the use of a linearized model, while all simulations of the crane behavior are based on the 3D nonlinear model. The results of open-loop and closed-loop experiments are discussed.

## Laboratory model of 3D crane

The results presented in this paper concern a laboratory model of gantry crane, manufactured by the Inteco Co. Ltd. (Fig. 1). Although the laboratory crane is not a copy of a real industrial one, in many aspects its behavior is similar [13].

The model is 1 m long, 1 m high and the payload may be hoisted up to 1 m. The mass of the payload is equal to 1 kg. The cart can move in two directions. Its position is measured by two encoders. The payload may be shifted up or lowered, with the length of the rope measured by an encoder. The cart has a mechanical unit mounted, which measures two angles of the payload with the use of two encoders.

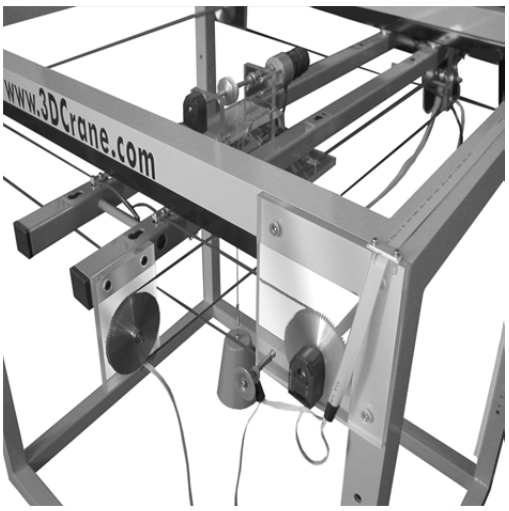


Fig.1 The laboratory crane model

The angles describe the position of the payload referenced to the cart. The crane has three DC motors installed, two for driving the cart and one for hoisting the payload. The motors are controled from a PC computer . The system is integrated with the Simulink environment. Some issues concerning vlocity control of the crane are considered in [13].

## Mathematical model

Figure 2 presents forces acting in the crane system. It is assumed that five quantities are accessible: $x_c$ denotes the position of the cart in the $x$ direction; $y_c$ denotes the position of the rail with the cart in the $y$ direction; $R$ denotes the length of the rope; $\alpha$ denotes the angle between the $x$ axis and the lift-line; $\beta$ denotes the angle between the negative direction on the $z$ axis and the orthogonal projection of the lift-line onto the $yz$ plane.

The Cartesian coordinates of the payload are denoted by $x_p$, $y_p$ and $z_p$. Denote the mass of the payload by $m_p$, the mass of the cart by $m_c$, and the mass of the moving rail by $m_r$. $F_x$ is the control force driving the cart along the rail, $F_y$ is the control force driving the rail with cart in the $y$ direction (perpendicularly to the rail), and $F_R$ is the force controlling the length of the lift-line. The respective friction forces are denoted by $T_x$, $T_y$, and $T_R$.

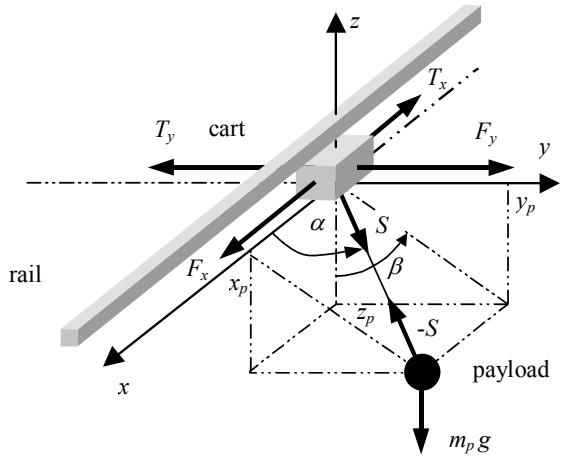


Fig. 2. Forces acting in the 3D crane system

It is assumed that the friction is proportional to the respective velocity component

$$T_x = k_1 m_c \dot{x}_c\,, \quad T_y = k_2 (m_c + m_r)\dot{y}_c\,, \quad T_R = k_3 m_p \dot{R}\,.$$

The controls are connected with the control forces by the relationships

$$(1) \qquad u_1 = \frac{F_x}{m_c}, \quad u_2 = \frac{F_y}{m_c + m_r}, \quad u_3 = \frac{F_R}{m_p}.$$

The resulting set of equations is solved with respect to second derivative of: $x_c$, $y_c$, $R$, $\alpha$ and $\beta$. To this end define state variables and introduce some auxiliary notations

$$x_1 = x_c \qquad x_6 = \dot{x}_5 = \dot{\alpha} \qquad s_n \equiv \sin x_n$$
$$x_2 = \dot{x}_1 = \dot{x}_c \qquad x_7 = \beta \qquad c_n \equiv \cos x_n$$
$$x_3 = y_c \qquad x_8 = \dot{x}_7 = \dot{\beta}$$
$$x_4 = \dot{x}_3 = \dot{y}_c \qquad x_9 = R$$
$$x_5 = \alpha \qquad x_{10} = \dot{x}_9 = \dot{R}$$

$$V_5 = c_5 s_5 x_8^2 x_9 - 2x_{10}x_6 + g c_5 c_7$$
$$V_6 = 2x_8(c_5 x_6 x_9 + s_5 x_{10}) + g s_7$$
$$V_7 = s_5^2 x_8^2 x_9 + g s_5 c_7 + x_6^2 x_9$$
$$\mu_1 = \frac{m_p}{m_c}, \qquad \mu_2 = \frac{m_p}{m_c + m_r}.$$

. The symbol of the state variables may collides with the notation of the $x$ direction in the Cartesian system but the author decided not to change this because the meaning of the variables always stems from a context and this depiction is popular among engineers.

The reduced controls, with the friction terms subtracted, are defined by

$$N_1 = u_1 - k_1 x_2, \quad N_2 = u_2 - k_2 x_4, \quad N_3 = u_3 - k_3 x_{10}\,.$$

Finally the ten state equations describing the dynamics of the crane are as follow

$$(2) \qquad \dot{x}_1 = x_2$$
$$\dot{x}_2 = N_1 + \mu_1 c_5 N_3$$
$$\dot{x}_3 = x_4$$
$$\dot{x}_4 = N_2 + \mu_2 s_5 s_7 N_3$$
$$\dot{x}_5 = x_6$$
$$\dot{x}_6 = \left(s_5 N_1 - c_5 s_7 N_2 + (\mu_1 - \mu_2 s_7^2) c_5 s_5 N_3 + V_5\right) \Big/ x_9$$
$$\dot{x}_7 = x_8$$
$$\dot{x}_8 = -(c_7 N_2 + \mu_2 s_5 c_7 s_7 N_3 + V_6)/(s_5 x_9)$$
$$\dot{x}_9 = x_{10}$$
$$\dot{x}_{10} = -c_5 N_1 - s_5 s_7 N_2 - (1 + \mu_1 c_5^2 + \mu_2 s_5^2 s_7^2) N_3 + V_7$$

The values of the parameters obtained by identification experiments are as follows:

$$m_p = m_r = 1\,\text{kg},\ m_c = 14\,\text{kg},$$
$$k_1 = 350\,\text{s}^{-1},\ k_2 = 375\,\text{s}^{-1},\ k_3 = 416\,\text{s}^{-1}.$$

A more detailed description of the mathematical model may be found in [14]

**Time-optimal experiment**

Classic crane control consists of three phases.

- Starting phase. The cart is accelerated and the payload shifted up. Oscillations of the payload should be minimized and the crane should be prepared to the second phase.
- Transport phase. The payload is moved (with constant speed) to a vicinity of the desired position.
- Terminal phase. The payload is put down, the crane stopped and the oscillations damped.

The experiment presented below consists only of the starting phase and the terminal phase. The middle phase is omitted because the respective control problem is less interesting in our setting. The control task in the first part of the experiment is to steer the crane from a point $A$ in the state space, with

$$(3) \quad x_c = -0.425\ \text{m},\ y_c = 0.2\ \text{m},\ \alpha = \tfrac{1}{2}\pi\ \text{rad},\ R = 0.7\ \text{m}$$

(only nonzero state components are shown), to a point $B$ with

$$(4) \quad x_c = -0.2\ \text{m},\ y_c = 0.2\ \text{m},\ \dot{y}_c = 0.1\ \text{m/s},\ \alpha = \tfrac{1}{2}\pi\ \text{rad},\ R = 0.5\ \text{m}.$$

At the end of the first phase, the payload should hang vertically without oscillations and the cart with payload should move in the *y* direction with the transportation speed of 0.1 m/s. Note that that the payload is shifted up to a desired height.

Point $B$ is the initial state for the second phase of the experiment. The control task is to move the payload to a destination point, to stop the crane and to eliminate oscillations generated by the braking cart. This phase should end at the target state *C* where

$$(5) \quad x_c = -0.2\ \text{m},\ y_c = 0.45\ \text{m},\ \alpha = \tfrac{1}{2}\pi\ \text{rad},\ R = 0.7\ \text{m}.$$

At $C$, the cart is stopped. The payload is lowered to the original height and its oscillations are damped.

The time-optimal controls have been calculated for both phases, for bounded control forces:

$$|F_x| \le 54.5\ \text{N},\ |F_y| \le 60\ \text{N},\ \text{and}\ F_R \in [-9.8, 29.4]\ \text{N}.$$

Figure 3 presents a selected time-optimal control $F_x$ which moves the payload in $x$ direction from point $A$ through point $B$ to point $C$. Figure 4 shows the motion of the payload (angle α ) when the calculated time-optimal control forces are fed to the real crane. Dotted line shows the time-optimal

trajectory. It can be seen that the results of the open-loop control in the laboratory system are in fairly good accordance with the assumptions (4) and (5). The time-optimal experiment more detailed presented may be found in [15].

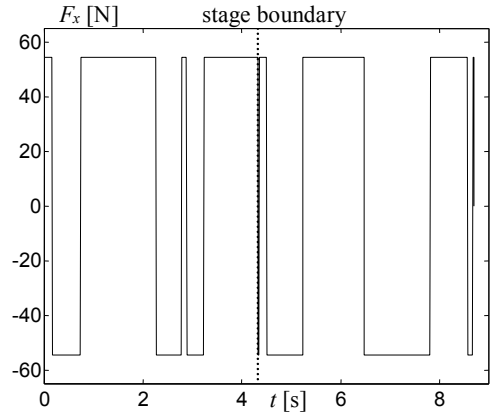


Fig. 3. Control force in *X* direction

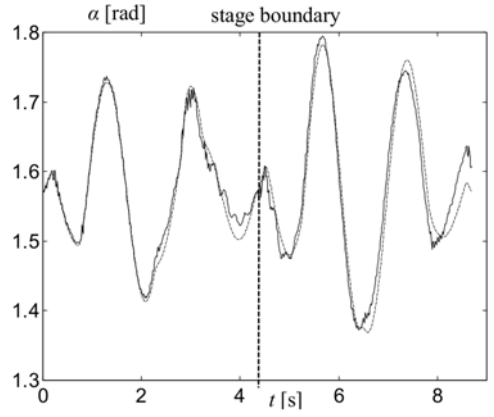


Fig. 4. Movement of payload – angle $\alpha$, simulation result – dotted line, open-loop experiment – solid line

**Optimal LQ Controller**

The aim of this section is to present a way of constructing a control algorithm which solves the problem of tracking a desired trajectory. All deviations from the desired trajectory, which may differ from the reference trajectory, should be eliminated optimally according to a performance index $S$.

The Linear Quadratic (LQ) controller is a solution of the optimal control problem for linear systems with a quadratic performance index. Therefore, a model linearized around the reference trajectory $\bar{x}$ and reference control $\bar{u}$ has to be used. The linearized model is valid only in a sufficiently small neighborhood of the reference trajectory, so the LQ controller works properly only in that neighborhood.

Static friction is omitted in the construction of the LQ controller. To obtain exactly the same trajectories in the presence of static friction as in the model without it, the calculated control $u_1$ should be replaced with $u_1+T_{s1}\mathrm{sgn}x_2$, the control $u_2$ with $u_2+T_{s2}\mathrm{sgn}x_4$, and the control $u_3$ with $u_3$ - $T_{s3}\mathrm{sgn}x_{10}$. In practice, the term $\mathrm{sgn}x_2$ is replaced with $\mathrm{sgn}u_1$, $\mathrm{sgn}x_4$ with $\mathrm{sgn}u_2$, and $\mathrm{sgn}x_{10}$ with -$\mathrm{sgn}u_3$. Because of the small inertia of the cart the errors caused by this simplification can be neglected.

Below, a linear-quadratic controller is constructed. It makes the system track the so called desired trajectory. It is possible to change the reference trajectory at the construction stage according to one's requirements. This modification determines the desired trajectory.

Let us write down the 3D crane equations in the following general form

$$\dot{x}(t) = f(x(t),u(t)), \quad t \in [0,T] \tag{6}$$
$$x(t) \in \Re^{10}, \quad u(t) \in \Re^{3}.$$

The initial state is given by

$$x(0) = x_0. \tag{7}$$

The reference trajectory

$$\bar{x} : [0,T] \to \Re^{10}$$

and reference control

$$\bar{u} : [0,T] \to \Re^{3}$$

are also given. Both the reference vectors are obtained as simulation results, so they fulfill (6). Define the deviations of state and control, $\Delta x = x - \bar{x}$ and $\Delta u = u - \bar{u}$. The linearized system, determined at the reference point has the form

$$\Delta\dot{x}(t) = A(t)\Delta x(t) + B(t)\Delta u(t), \quad t \in [0,T] \tag{8}$$

where

$$A(t) = \frac{\partial f\left(\bar{x}(t),\bar{u}(t)\right)}{\partial x(t)}, \quad B(t) = \frac{\partial f\left(\bar{x}(t),\bar{u}(t)\right)}{\partial u(t)}.$$

A reduction of unwanted properties of the reference trajectory $\bar{x}$ (e.g., too great oscillations of the payload) may be achieved thanks to the appropriate construction of the quadratic performance index $S$

$$S(\Delta u) = y(T)^{\mathsf{T}} P y(T) + \int_0^T \left( y(t)^{\mathsf{T}} Q y(t) + \Delta u(t)^{\mathsf{T}} V \Delta u(t) \right) \mathrm{d}t \tag{9}$$

$$y(t) = \Delta x(t) - z(t) \tag{10}$$

The function $z(t)$ is chosen in such a way that

$$\bar{x}(t) + z(t)$$

is the desired trajectory. Assume

$$P = P^{\mathsf{T}} \geq 0\,, \; Q = Q^{\mathsf{T}} \geq 0 \text{ and } V = V^{\mathsf{T}} > 0\,.$$

The unique optimal control deviation $\Delta u^*(t)$ which minimizes the performance index (9) on the trajectories of (8), and the corresponding optimal state deviation $\Delta x^*(t)$ fulfill the equality

$$\Delta u(t)^* = -V^{-1}B(t)^{\mathsf{T}}\left(K(t)\Delta x^*(t) + k(t)\right), \quad t \in [0,T] \tag{11}$$

$K(t)$ is a symmetric, positive semidefinite 10 x 10 matrix which is a solution of the Riccati equation

$$\dot{K} = KBV^{-1}B^{\mathsf{T}}K - KA - A^{\mathsf{T}}K - Q, \quad t \in [0,T] \tag{12}$$

with the final condition $K(T) = P$. The vector function $k(t)$ is a solution of the equation

$$\dot{k} = (KBV^{-1}B^{\mathsf{T}} - A^{\mathsf{T}})k + Qz, \quad t \in [0,T] \tag{13}$$

with the final condition $k(T) = -Pz(T)$.

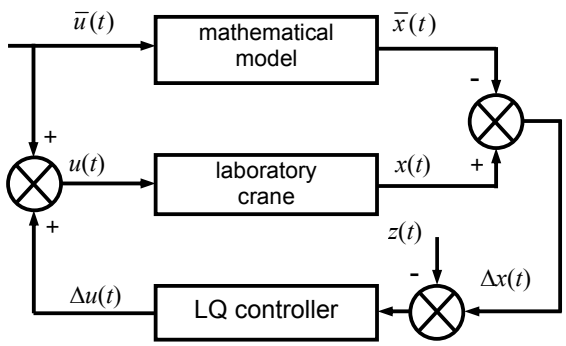


Fig. 5. Appliance of the linear-quadratic controller.

The reference trajectory $\bar{x}$ and the reference control $\bar{u}$ have been obtained in the simulation of the system (6). The reference control $\bar{u}$, fed into the laboratory crane makes the model move along a trajectory which is similar to $\bar{x}$. Practically, both trajectories always differ. Figure 5. presents the idea of using the linear-quadratic controller.

**Robustification of Time-optimal Trajectory with the LQ Controller**

Robustification of the time-optimal trajectory relies on tracking it with an LQ controller and optimal elimination of all deviations from the desired trajectory. Optimally, means according to the performance index $S$ (9). The performance index $S$ is constructed in such a way that it gives a possibility to change the reference trajectory (in this case time-optimal) to a desired trajectory (10).

In the experiment presented below, the controller follows the desired trajectory, which is modified by the function $z(t)$ (10) in order to avoid oscillations of the payload. The controller "tries" also to stabilize the payload, even if it should swing according to the reference trajectory. Oscillations in the reference trajectory are presented below in Figures 14 and 15.

**Construction of the controller.**

At the beginning of the experiment the matrix $K(t)$ (12) and the vector $k(t)$ (13) were calculated off-line for a unit matrix $V$ and

(14)
$$Q = \mathrm{diag}(900, 100, 900, 100, 300, 6, 300, 6, 2\cdot 10^6, 5000)$$

The weights in the matrix $Q$ are lowered to 100 for the cart velocity components and to 6 for the angular velocities of the payload. This is caused by the poor quality of the velocity signals. They are thus almost totally eliminated from the control process.

The much higher values of $Q_9$ and $Q_{10}$ than the values of other components of the diagonal of $Q$ are due to the model scale. To explain this, write the optimal control correction corresponding to a state deviation $\Delta x$ in the form $\Delta u = -W\Delta x - w$ where $W(t)=V^{-1}B(t)^{\mathrm{T}}K(t)$ and $w(t)=V^{-1}B(t)^{\mathrm{T}}k(t)$. Let us first consider the control correction caused by an error equal to 1 cm in the rope length. We neglect its first two components as $|W_{13}|$ and $|W_{23}|$ are much less than $|W_{33}|$ (see Fig. 10). Hence $\Delta u_3 = -W_{33}\Delta x_9 - w_3 \approx -14 - w_3$. After rescaling by $m_c$, we obtain $\Delta F_R \approx -14 - w_3$ [N]. Suppose now a similar error in the cart position, $\Delta x_1$=0.01m, with other state deviations equal to zero. Since $|W_{21}|$ and $|W_{31}|$ are much less than $|W_{11}|$ (see Fig. 7), we neglect two last components of the corresponding control correction. The first component is $\Delta u_1 = -W_{11}\Delta x_1 - w_1 \approx -0.3 - w_1$. After rescaling by the factor $m_w$=14kg, we get $\Delta F_x \approx -4.2 - 14w_1$ [N]. The weights $Q_9=2\cdot 10^6$ and $Q_1$=900 give similar corrections of the control forces $F_R$ and $F_x$ for a 1 cm error of the corresponding state deviations. Analogously, the deviations of the angles $\alpha$ and $\beta$ equal to 0.02 rad cause similar force corrections, respectively $\Delta F_x \approx -5.6 - 14w_1$ [N] and $\Delta F_y \approx -6 - 15w_2$ [N].

The function $z(t)$ which defines the desired trajectory is assumed as follows

(15)
$$z = (0, 0, 0, 0, \tfrac{\pi}{2} - \bar{x}_5, -\bar{x}_6, -\bar{x}_7, -\bar{x}_8, 0, 0)^{\mathrm{T}}.$$

This means that no changes are introduced to the cart movement and rope length, but the desired angle $\alpha$ is equal to $\pi/2$, the desired angle $\beta$ is 0 and the desired angular velocities are equal to zero.

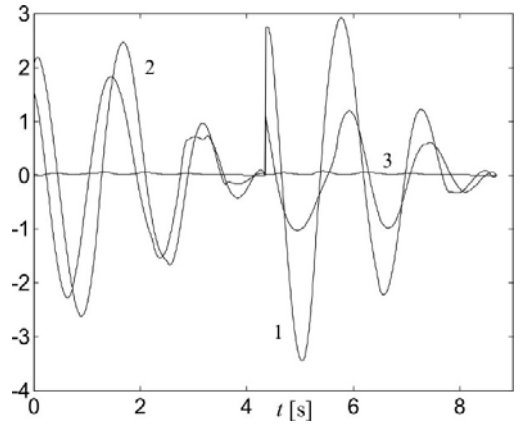


Fig. 6. Vector $B(t)^{\mathrm{T}}k(t)$, numbers denote vector components

Figure 6 presents the calculated vector $B(t)^{\mathrm{T}}k(t)$ that appears additively in the right-hand side of the control formula. The values of the vector are determined by the desired trajectory. If the desired trajectory were equal to the reference one, the vector $k(t)$ would be equal to zero.

Figures 7 – 10 present four chosen columns of the matrix $B(t)^{\mathrm{T}}K(t)$. The first column of the control matrix (Fig.7) is responsible for controlling the cart motion in the $x$ direction.

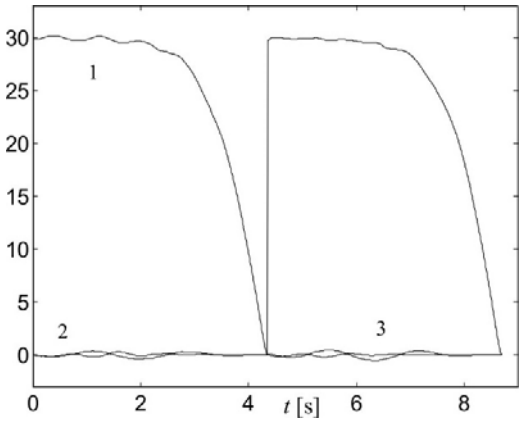


Fig. 7. Column 1 of $B(t)^{\mathrm{T}}K(t)$

The first component of the column, which influences $\Delta u_1$ after multiplication by $\Delta x_1$, has the biggest value. Other components have a weak effect on the movement in this direction. Similarly, the first component in column five has the biggest value (Fig.9). It is responsible for tracking the angle $\alpha$, which depends on the control in the $x$ direction. The third column shown in Figure 8 is responsible for the cart movement in the $y$ direction and has the second component the biggest. The ninth column (Fig.16) controls the rope length, so the third component is the biggest.

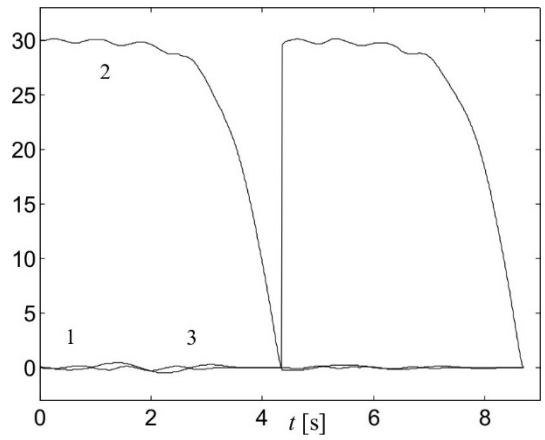


Fig. 8. Column 3 of $B(t)^{-1}K(t)$

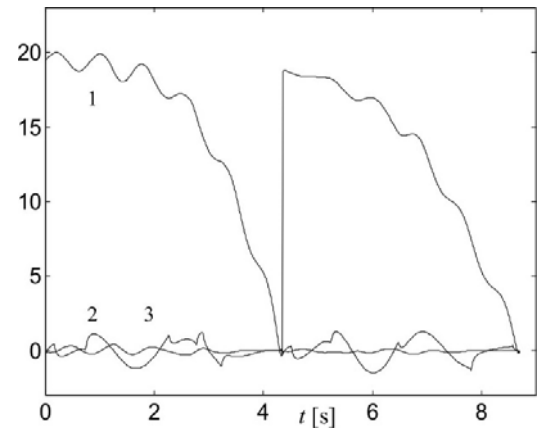


Fig. 9. Column 5 of $B(t)^{-1}K(t)$

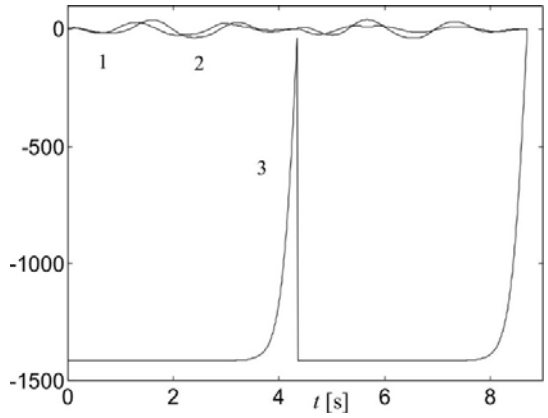


Fig. 10. Column 9 of $B(t)^{-1}K(t)$

**Experiment.**

The LQ controller presented above was applied in the laboratory crane model according to the scheme in Figure

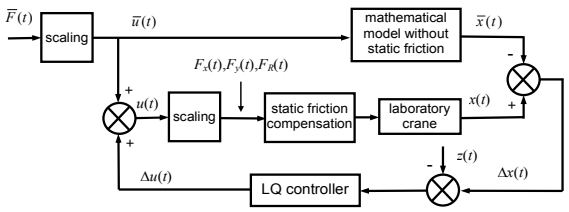


Fig 11. Block diagram of the control loop with LQ controller

The LQ controller is based on the mathematical crane model which does not include static friction, therefore it is necessary to compensate it. Thanks to the compensation block, the laboratory model behaves (for the LQ controller) like an object without static friction. Since the control $\Delta u$ is calculated for the scaled model, a scaling block has also to be added to obtain the control forces $F_x$, $F_y$, $F_R$.

Figures 12 – 19 present results of the closed loop experiment with the LQ controller constructed according to the above assumptions. Although the desired movement of the cart is the same as the reference one, both trajectories differ clearly. The differences come from the vector $V^{-1}B(t)^{\mathrm{T}}k(t)$ which is added to minimize the payload swings.

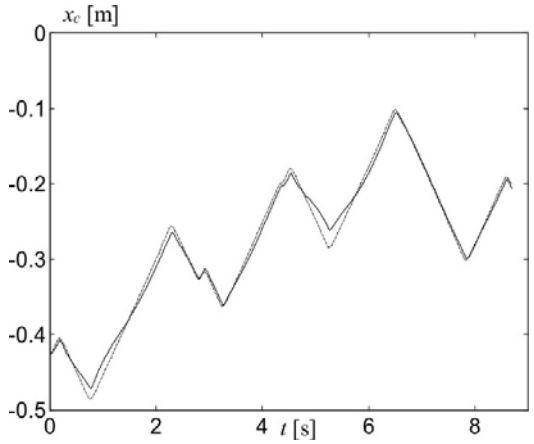


Figure 12. Movement of the cart in *x* direction, reference trajectory – dotted line

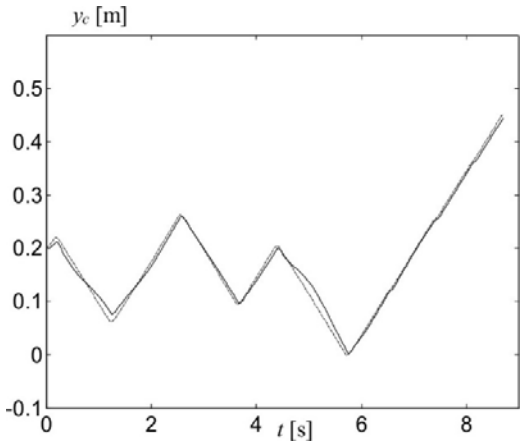


Fig. 13. Movement of the cart in $y$ direction, reference trajectory – dotted line, closed-loop experiment – solid line

The payload is swinging less in the closed-loop experiment than in the open loop one (Fig. 14 and 15). It also swings less than in the reference trajectory.

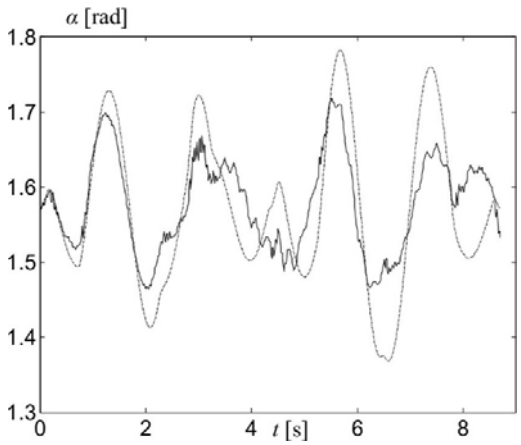


Fig. 14. Angle $\alpha$, open-loop experiment – dotted line, closed-loop experiment – solid line

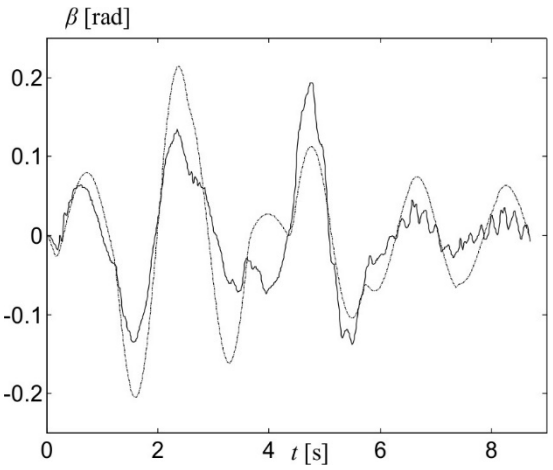


Fig. 15. Angle $\beta$, open-loop experiment – dotted line, closed-loop experiment – solid line

Let us introduce indexes which help to estimate the controller effectiveness. For the angle $\beta$ and for the angle $\alpha$

$$S_{\text{ang}} = \int_0^{8.7} |\beta(t)|\,\mathrm{d}t \quad S_{\text{ang}} = \int_0^{8.7} |\alpha(t) - \tfrac{\pi}{2}|\,\mathrm{d}t$$

.

The smaller value of the index, the smaller swings of the payload. Table 1 contains values of the calculated performance index for the reference, open-loop and closed-loop trajectories. The results show good effectiveness of the LQ controller which is equal to 34.2% for the angle $\alpha$ and 25.7% for the angle $\beta$.

Tab. 1. Values of the performance index $S_{\text{ang}}$ for the angles $\alpha$ and $\beta$

| | $S_{\text{ang}}$ for reference trajectory | $S_{\text{ang}}$ for open-loop experiment | $S_{\text{ang}}$ for closed-loop experiment |
|---|---|---|---|
| $\alpha$ | 0.7183 (100%) | 0.6894 (96%) | 0.4725 (65.8%) |
| $\beta$ | 0.5879 (100%) | 0.6102 (103.8%) | 0.437 (74.3%) |

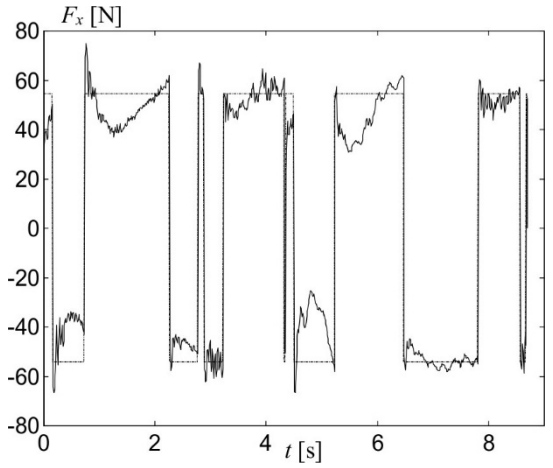


Fig. 16. Control force $F_x$, reference trajectory – dotted line, closed-loop experiment – solid line

Figures 16, 17 and 19 show changes made in the control forces by the controller. The smallest corrections were made to the $F_R$ force, and the rope length is very well tracked (Fig. 18 – differences are difficult to notice). Bigger improvements of the $F_x$ and $F_y$ forces are caused by the desired $\alpha$ and $\beta$ trajectories which seriously differ from the reference ones.

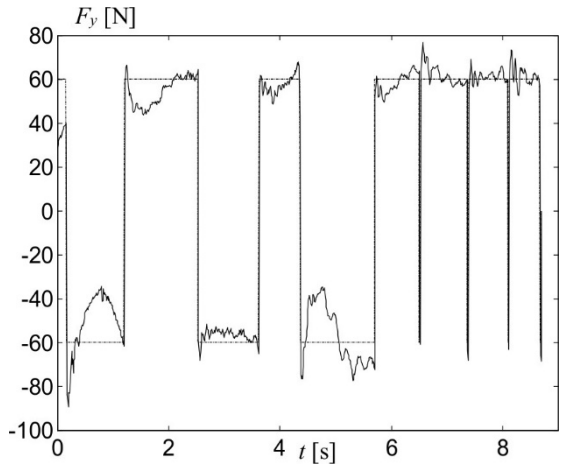


Fig. 17. Control force $F_y$, reference trajectory – dotted line, closed-loop experiment – solid line

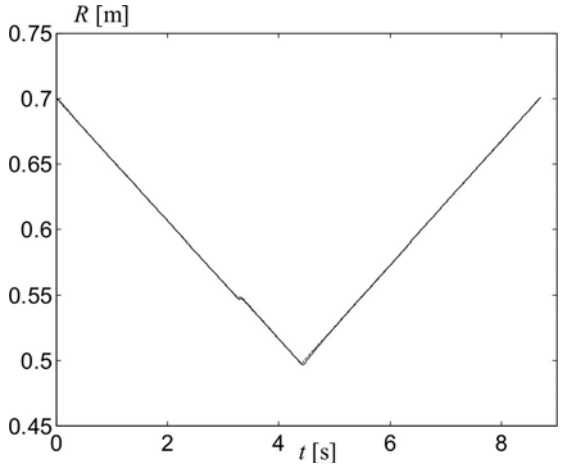


Fig. 18. Control force $F_x$, reference trajectory – dotted line, closed-loop experiment – solid line

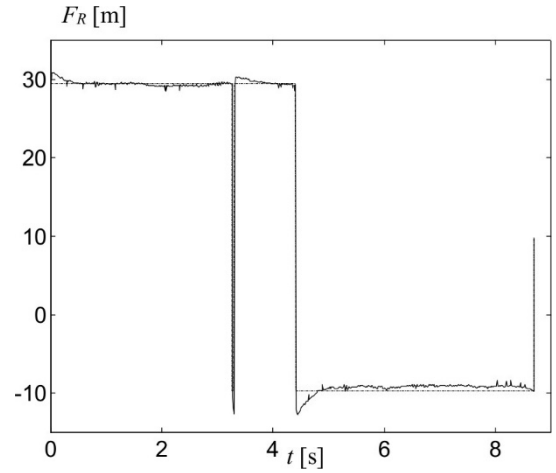


Fig. 19. Control force $F_R$, reference trajectory – dotted line, closed-loop experiment – solid line

**Conclusions**

The presented mathematical model of 3D crane requires a lot of numerical calculations, but the quality of the model allows construction of very effective controllers. Furthermore, at the present time when the PC based on core i7 becomes a standard machine, the complication of the model is no longer a problem. The physical character of the model equations allows the identification process to be done in a simple, intuitive and fast way.

The simulations and experiments show that it is possible to control the crane in a time-optimal way basing on its mathematical model. Usually, such controls contain many switches. This feature is responsible for generating oscillations of the payload during the shifting up or lowering phase.

The proposed LQ control algorithm partly resolves the problem of oscillations. After its implementation for tracking the desired trajectory the oscillations are reduced by 25% to 35%. Of course, the presented method changes the time-optimal control to suboptimal. How much the new control becomes suboptimal, depends on the force margin that is assumed for the controller. The more accurate model and smaller level of noise, the smaller force margin is needed.

A more effective way of tracking the desired trajectory might be an algorithm which changes the switching times, but this algorithm does not resolve the problem of swinging payload, which is critical for cranes.

*The paper was financed under statutory activities 11.11.120.396*

***Autor**: dr inż. Mariusz Pauluk, AGH University of Science and Technology, Department of Automation and Biomedical Engineering, al. Mickiewicza 30, 30-059 Kraków, E-mail: mp@agh.edu.pl*

REFERENCES

[1] Najib K., Dankadai, Ahmad 'Athif Mohd Faudzi, Amir Bature, Suleiman Babani, Muhammad I. Faruk, Position Control of a 2D Nonlinear Gantry Crane System using Model Predictive Controller, *Applied Mechanics and Materials*, Vol. 735 (2015) 282-288

[2] Yoshida K., Nonlinear Controller Design for a Crane System with State Constraints, *proceedings of the American Control Conference* (1998), Philadelphia, Pennsylvania

[3] Hong KS, Kim JH, Lee KI, Control of a Container Crane: Fast Traversing and Residual Sway Control from the Perspective of Controlling an Undeactuated System, *proceedings of the American Control Conference, Philadelphia* (1998)*, Pennsylvania*

[4] Tuan Anh Le ,Soon-Geul Lee and Sang-Chan Moon, Partial feedback linearization and sliding mode techniques for 2D crane control, *Transactions of the Institute of Measurement and Control* (2014), Vol. 36(1) 78–8

[5] Yoshida Y., Tsuzuki K., Visual Tracking and Control of a Moving Overhead Crane Load, Advanced Motion Control, (2006), 630 – 635, 9th IEEE International Workshop on,

[6] Liu Yong-qiu , Liu Xiao-feng , Wang Hai-xia, Strategic Analysis and Experimental Research on Synchronization Control of Dual-motor in Crane, *Applied Mechanics and Materials* Vols. 644-650 (2014) pp 836-839

[7] Hämäläinen J.J., A.Martinnen, L.Baharova, J.Virkunen, Optimal path planning for a trolley crane: fast and smooth transfer of load, *IEE Proceedings Control Theory* (1995) *Appl.*, Vol. 142, No. 1

[8] Turnau A. Postępy w regulacji optymalnoczasowej w czasie rzeczywistym, *Automatyka i Robotyka*, *Akademicka Oficyna Wydawnicza EXIT*, Warszawa (2013), ISBN 978-83-7837-032-1.

[9] Korytowski A., M. Szymkat, Consistent Control Procedures in the Monotone Structural Evolution. Part 1: Theory, *Recent Advances in Optimization and its Applications in Engineering.* Ed. by M. Diehl et al., Springer, (2010), 247-256.

[10] Szymkat M. A. Korytowski, Consistent Control Procedures in the Monotone Structural Evolution. Part 2: *Examples and Computational Aspects. Recent Advances in Optimization and its Applications in Engineering*. Ed. by M. Diehl et al., Springer, 2010, 257-266

[11] Szymkat M, Korytowski A, Turnau A.,Variable control parameterization for time-optimal problems, *IFAC CACSD 2000 Conference*, Salford, UK

[12] Pesch H.J., Real-time Computation of Feedback Controls for Constrained Optimal Control*Problems,* Part1: Neighbouring Extremals, *Optimal Control Applications and Methods 10* (1989), 129-145

[13] Pauluk M., Projektowanie algorytmów sterujących w układach sterowanych napięciowo i prądowo, *Miesięcznik Naukowo-Techniczny PAR – Pomiary, Automatyka, Robotyka* (2005)*,* 12/2005, 37-45, Warszawa

[14] Pauluk M., Model matematyczny trójwymiarowej suwnicy, *"Automatyka"* – półrocznik tom 6, zeszyt 1 (2002), 69-102, Akademia Górniczo - Hutnicza, Kraków

[15] Augustyn J., Bania P., Baranowski J., Czubak P., Długosz M., Klemiato M., Pauluk M., Skruch P., Tutaj A., Perspektywiczne zagadnienia automatyki i robotyki, Baranowski J. (ed). w przygotowaniu do druku